Natural Convection Along a Wedge

L. S. Yao*
Arizona State University, Tempe, Arizona

The separation of the natural-convection boundary layers near the tip of a vertical wedge is analyzed. The boundary layer becomes inviscid, but rotational near the tip. An induced pressure gradient in this flow region responds to the upstream transmission of the downstream geometry change. Large temperature and velocity gradients are induced across the thin viscous layer near the solid surface. This causes a substantial modification of the local heat-transfer rate and wall shear stress. This two-layer structure (double decks) connects the natural-convection boundary layers with the thermal plume above the wedge. It is shown that the determination of the proper matching condition, which aligns the natural-convection boundary layers with the thermal plume, is the crucial step in solving this problem.

Nomenclature

a = constant, Eq. (13)
A = displacement, Eq. (17)
b = constant, Eq. (26)
f = stream function, Eq. (4)
g = gravitational acceleration
h = temperature function, Eq. (26)
Gr = Grashof number, Eq. (1)
ℓ = wedge height
k = thermal diffusivity
Nu = Nusselt number
P = pressure
Pr = Prandtl number
Q = total heat flux
T = temperature
x, y = coordinates
u, v = velocities
α = tanφ
β = thermal diffusivity
ϵ = small parameter, Eq. (1)
η = boundary-layer coordinate, Eq. (4)
δ = displacement, Eq. (1)
θ = dimensionless temperature, Eq. (1)
ν = kinematic viscosity
ρ = density
τ = shear stress
ϕ = half-wedge angle
ψ = stream function, Eq. (7)

Subscripts
b = natural-convection boundary layer
p = thermal plume
l = double decks

I. Introduction

SEPARATION is a natural flow phenomenon. In spite of its importance, our understanding of the associated physics is limited. This is mainly because the boundary-layer concept cannot be applied to separated flows. Consequently, the major dimensionless parameters for the problem are still unknown.

In this paper, we study a special kind of flow separation and the corresponding heat-transfer mechanism. This type of flow separation can be described as the *collision* of two natural-convection boundary layers (or two wall jets). Unlike a forced-flow separation, no recirculating-flow region has been observed below the main boundary layers. Examples include flows near the equator of a spinning sphere,[1,2] natural-convection boundary layers near the top of a blunt body[3-5] or in a cavity, and secondary boundary layers near the inner bend of a curved pipe[6-8] or near the top of a heated straight pipe.[9] At present, a complete structure of those "head-on" colliding flows is unavailable. Natural convection along a vertical wedge (see Fig. 1), a simple version of such flows, is studied in order to gain insight into this important phenomenon.

Three flow regions can be identified for the problem: thermal boundary layers, near plume, and double decks (Fig. 1). Since the boundary layers and the near plume are governed by parabolic differential equations, a transition region is needed to join them smoothly. This transition region provides the space required for the flow to adjust to the geometric change and consists of two layers or *double decks*. In the main deck, away from the surface of the wedge, a pressure gradient is induced by the local flow adjustment. This induced pressure gradient is the mechanism by which the influence of the geometry change is transmitted *upstream*. The existence of a lower deck, a thin layer near the surface of the wedge, allows the fluid to satisfy the boundary conditions on the surface. Large temperature and velocity gradients across the lower deck influence the local heat-transfer rate and wall shear stress.

The double-deck structure[10,11] shows that a disturbance inside a boundary layer can have an upstream influence to a distance of $O(\epsilon^{6/7})$, where $\epsilon = Gr^{-1/4}$ (for thermal boundary layers) or $Re^{-1/2}$ (for wall jets). Messiter[10] used the natural-convection boundary layer along a finite vertical plate as a model problem to show, by this double-deck structure, that the boundary-layer solution on the plate can smoothly join the thermal-plume solution[12] above the plate. The structure of the double deck shares many similarities with the triple-deck structure near the trailing edge of a flat plate in a uniform stream.[13,14] Smith and Duck[11] were interested in developing a general theory to describe the collision of two nonparallel wall jets. They conjectured that the main boundary layer separates at a distance $O(Re^{-3/14})$ from the location of the collision and a relatively large recirculating flow exists below the main boundary layer. On the other hand, such a recirculating flow has not been identified in the numerical solution of the collision of boundary layers near the equator of a spinning sphere[1,2] or in experiments on natural convection near the top of a blunt body.[3-5]

Presented as Paper 87-1590 at the AIAA 22nd Thermophysics Conference, June 8-10, 1987; received Oct. 13, 1986; revision received Jan. 23, 1987.

*Professor, Department of Mechanical and Aerospace Engineering.

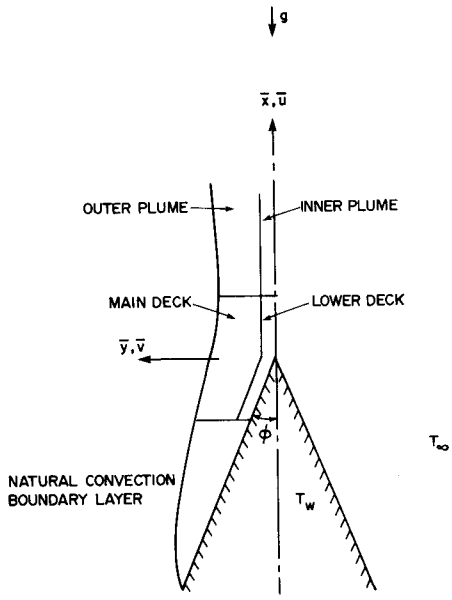

Fig. 1 Physical model and coordinates.

The first numerical solution of a double deck was obtained for a rotating disk,[15] a degenerate case of a rotating sphere. Two boundary layers meet at the edge of the disk and form a free-boundary flow. Since the boundary layers are parallel and do not collide, no recirculating-flow region exists. This problem is similar to the problem of natural convection along a vertical finite plate, as formulated in Ref. 10 and solved in Ref. 16.

Subsequently, Merkin and Smith[17] studied natural-convection boundary layers near a corner or the trailing edge of a vertical wedge. They formulated the equations of a double-deck structure for corners whose angles differ slightly from 180 deg or for wedges of very small angles. Their solutions show that a recirculating-flow region exists even for these two limiting cases, which is not consistent with expectation. In particular, no unfavorable pressure gradient is induced by a thermally-driven boundary layer, so a recirculating-flow region is unlikely to exist, and, moreover, has never been observed. Thus, the validity of the proposed double-deck structure has been in doubt.

Later, it was demonstrated[18] that the double deck is indeed a proper flow structure, at least for a non-head-on collision of two boundary layers. The key step in formulating the problem in order to obtain a correct solution is to choose a proper coordinate system. In this paper, we discuss the details of the heat-transfer mechanism associated with such flows. The extended Prandtl's coordinates,[19] which were found to be suitable for the problem, are described in Sec. II. Section III briefly summarizes the structure of the natural-convection boundary layers on the wedge in the nonorthogonal Prandtl's coordinates and shows that the results agree completely with those obtained by solving the equations in the conventional body coordinates. In Sec. IV, we show that Yang's solution[12] of the thermal plume above a vertical plate can be directly applied to the wedge problem with a different initial velocity profile. This shows that the near-plume structures downstream of a heated body are all alike. The solutions of the natural-convection boundary layers and the near plume provide the required matching conditions for the double-deck equations derived in Sec. V. Major results are presented and discussed in Sec. VI with a conclusion.

II. Formulation

Cartesian coordinates $(\bar{x}, \bar{y})$ are used, with $(\bar{u}, \bar{v})$ the corresponding velocity components. The $\bar{x}$ axis is aligned with the direction of gravity and the axis of the wedge. The half-wedge angle is denoted by $\phi = \tan^{-1}\alpha$, and the height of the wedge is ℓ (see Fig. 1). The wall temperature is held at T_w and the ambient temperature is T_∞.

Since the details of the extension of Prandtl's transportation theorem have been discussed in Refs. 18 and 19, a brief summary is sufficient. The dimensionless variables in Prandtl's coordinates are defined by

$$\hat{x} = \frac{\bar{x}}{\ell}, \qquad \hat{y} = \frac{\bar{y} - \delta(\bar{x})}{\ell} \qquad \text{(coordinates)}$$

$$\hat{u} = \frac{\bar{u}}{U_\infty}, \qquad \hat{v} = \frac{\hat{v} - \hat{\delta}_{,\hat{x}}\bar{u}}{U_\infty} \qquad \text{(velocity)}$$

$$\hat{P} = \frac{\bar{P} - \bar{P}_\infty}{\rho U_\infty^2} \qquad \text{(pressure)}$$

$$\hat{\theta} = \frac{T - T_\infty}{T_w - T_\infty} \qquad \text{(temperature)}$$

$$\epsilon^{-4} = Gr = \beta g_w (T - T_\infty)\ell^3/\nu^2 \qquad \text{(Grashof number)}$$

$$U_\infty = \nu/\ell\, Gr^{1/2} \qquad \text{(velocity scale)}$$

$$Pr = \nu/k \qquad \text{(Prandtl number)}$$

$$\hat{\delta} = \delta/\ell = \alpha\hat{x} = \begin{cases} 0, & \hat{x} > 0 \\ -\tan\phi\, \hat{x}, & \hat{x} < 0 \end{cases} \qquad \text{(displacement)} \qquad (1)$$

The dimensionless form of the equations of continuity, motion, and energy with the Boussinesqe approximation for density ρ are

$$\hat{u}_{,\hat{x}} + \hat{v}_{,\hat{y}} = 0$$

$$\hat{u}\hat{u}_{,\hat{x}} + \hat{v}\hat{u}_{,\hat{y}} = -\hat{P}_{,\hat{x}} + \hat{\delta}_{,\hat{x}}\hat{P}_{,\hat{y}} + \hat{\theta} + \epsilon^2[\hat{u}_{,\hat{x}\hat{x}} + (1 + \hat{\delta}_{,\hat{x}}^2)\hat{u}_{,\hat{y}\hat{y}} - 2\hat{\delta}_{,\hat{x}}\hat{u}_{,\hat{x}\hat{y}} - \hat{\delta}_{,\hat{x}\hat{x}}\hat{u}_{,\hat{y}}]$$

$$\hat{u}\hat{v}_{,\hat{x}} + \hat{v}\hat{v}_{,\hat{y}} + \hat{\delta}_{,\hat{x}\hat{x}}\hat{u}^2 = \hat{\delta}_{,\hat{x}}\hat{P}_{,\hat{x}} - (1 + \hat{\delta}_{,\hat{x}}^2)\hat{P}_{,\hat{y}} - \hat{\delta}_{,\hat{x}}\hat{\theta} + \epsilon^2[\hat{v}_{,\hat{x}\hat{x}} + (1 + \hat{\delta}_{,\hat{x}}^2)\hat{v}_{,\hat{y}\hat{y}} - 2\hat{\delta}_{,\hat{x}}\hat{v}_{,\hat{x}\hat{y}} - \hat{\delta}_{,\hat{x}\hat{x}}\hat{v}_{,\hat{y}} + \hat{\delta}_{,\hat{x}\hat{x}\hat{x}}\hat{u} + 2\hat{\delta}_{,\hat{x}\hat{x}}\hat{u}_{,\hat{x}} - 2\hat{\delta}_{,\hat{x}}\hat{\delta}_{,\hat{x}\hat{x}}\hat{u}_{,\hat{y}}]$$

$$\hat{u}\hat{\theta}_{,\hat{x}} + \hat{v}\hat{\theta}_{,\hat{y}} = \frac{\epsilon^2}{Pr}[\hat{\theta}_{,\hat{x}\hat{x}} + (1 + \hat{\delta}_{,\hat{x}}^2)\hat{\theta}_{,\hat{y}\hat{y}} - 2\hat{\delta}_{,\hat{x}}\hat{\theta}_{,\hat{x}\hat{y}} - \hat{\delta}_{,\hat{x}\hat{x}}\hat{\theta}_{,\hat{y}}] \qquad (2)$$

The subscript after a comma denotes a partial derivative. In transformed space, the wedge is represented by $\hat{y} = 0$ for $\hat{x} < 0$. This substantially simplifies the numerical procedure in solving the preceding equations.

III. Natural-Convection Boundary Layer

The scales for the natural-convection boundary layer are well-known: the thickness of the boundary layer and the normal velocity are $O(\epsilon)$. The boundary-layer coordinates are

$$x_b = 1 + \hat{x}, \qquad y_b = \hat{y}/\epsilon \qquad (3)$$

The expansions for velocity, pressure, and temperature are

$$\hat{u} = (1 + \alpha^2)(4x_b)^{1/2} f_b'(\eta_b) + \cdots$$

$$\hat{v} = -\epsilon(1 + \alpha^2)(4x_b)^{-1/4}(3f_b - \eta_b f_b') + \cdots$$

$$\hat{P} = 0 + \cdots$$

$$\hat{\theta} = \theta_b(\eta_b) + \cdots \qquad (4)$$

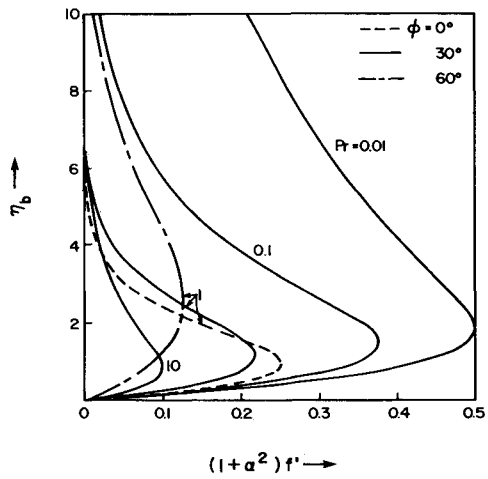

Fig. 2 Axial velocity of natural-convection boundary layer.

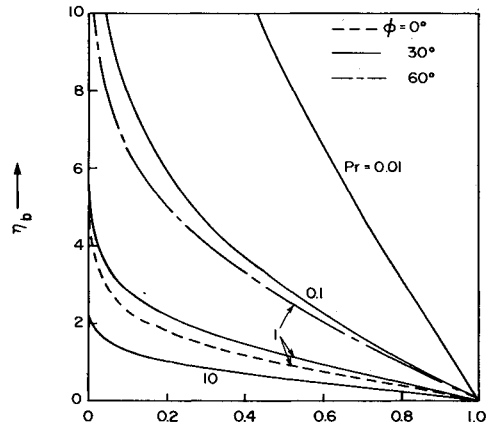

Fig. 3 Temperature distribution of natural-convection boundary layer.

where the subscript b is used to denote variables associated with the boundary layer and $\eta_b = y_b/(4x_b)^{1/4}$. The prime denotes a derivative with respect to η_b. The substitution of Eqs. (3) and (4) into Eq. (2), with terms of small orders neglected, yields the equations for the natural-convection boundary layer:

$$f_b''' + 3f_b f_b'' - 2f_b'^2 = \theta_b/(1+\alpha^2)^3$$

$$\frac{1}{Pr}\theta_b'' + 3f_b\theta_b' = 0 \tag{5}$$

The associated boundary conditions are

$$\eta_b = 0, f_b = f_b' = 0, \theta_b = 1 \quad \text{(wall condition)}$$

$$\eta_b \to \infty, f_b', \theta_b \to 0 \quad \text{(matching with quiescent ambient)} \tag{6}$$

The solutions of Eq. (5) satisfying Eq. (6) can be easily obtained by a numerical integration. Typical axial velocity profiles and temperature distributions for $Pr = 1$ and $\phi = 0$, 30, and 60 deg; $\phi = 30$ deg and $Pr = 0.01$, 0.1, 1, and 10 are given in Figs. 2 and 3. It is clear that the magnitude of the velocity decreases and the thickness of the boundary layer increases for wedges of larger angles. This is because the component of the buoyancy force parallel to the surface of the wedge decreases when the wedge angle increases. Consequently, the heat-transfer rate and wall shear stress are smaller for a larger wedge angle. The dependence on Prandtl number shows, as expected, that the boundary layer is thicker for smaller Pr, and the velocity is larger, but the heat-transfer rate is smaller.

In Prandtl's coordinates, the axial direction is not the direction parallel to the surface. Thus, the axial momentum equation is the projection of the momentum equation along the solid surface to this axis. One would expect that the solution of the axial momentum equation in Prandtl's coordinates might be restricted to the case of a small angle between the axial direction and the surface. Therefore, the natural-convection boundary-layer equations in the coordinates normal and parallel to the wedge are solved independently in order to find the restriction on Prandtl's transformation. The local wall heat flux and shear stress are compared. It is found that these two quantities, predicted by solving the equations in two different coordinates, agree for all wedge angles (up to 85 deg in our computations). This indicates that the axial momentum equation in Prandtl's coordinates is always valid, no matter how large the angle between the axial direction and the surface. Of course, one should recognize that Prandtl's transformation is singular for a wedge with a half-angle equal to 90 deg (a horizontal plane). This is why the current analysis is not valid for a head-on collision of two wall layers.

IV. Thermal Plume

The advantage of adopting Prandtl's coordinates is that the axial velocity of the natural-convection boundary layer is in line with that of the near plume, and the two velocities can readily be matched at $\hat{x} = 0$. Consequently, the distribution of velocity and temperature inside a thermal plume for small $\hat{x}$ is essentially similar to that above a vertical plate of finite length[12] but with a different initial condition. Since its structure is almost identical to the Goldstein near-wake solution[22] behind a flat plate, the near-plume solution consists of two layers, an inner plume and an outer plume. The solution form is briefly outlined in the following paragraphs.

The normal coordinate is defined as $y_p = \hat{y}/\epsilon$ to be consistent with the fact that the plume is thin. The appropriate expansions for small y_p (inner plume) are

$$\hat{\psi} = (3\hat{x})^{2/3}\lambda_1^{1/3} f_0(\eta) + \cdots$$

$$\hat{\theta} = 1 + (3\hat{x})^{1/3}\lambda_1^{-1/3}\mu_1 g_0(\eta) + \cdots \tag{7}$$

where

$$\eta = \lambda_1^{1/3} y_p/(3\hat{x})^{1/3}$$

$$\lambda_1 = \sqrt{2}\,(1+\alpha^2) f_b''(0)$$

$$\mu_1 = \frac{1}{\sqrt{2}}\theta_b'(0)$$

and $\hat{\psi}$ is the stream function introduced to satisfy the first of Eqs. (2). The governing equations for f_0 and g_0 can be obtained by substituting Eqs. (7) into Eqs. (2) and collecting terms of equal powers in $\hat{x}$. The result is

$$f_0''' + 2f_0 f_0'' - f_0'^2 = 0$$

$$\frac{1}{Pr} g_0'' + 2f_0 g_0' - f_0' g_0 = 0 \tag{8}$$

The prime denotes a derivative with respect to the appropriate independent variable.

The required conditions for the inner plume become

$$\eta = 0, \quad f_0 = f_0'' = g_0' = 0 \quad \text{(symmetry condition)}$$

$$\eta \to \infty, \quad f_0' \to \eta + a_1$$

$$g_0 \to \eta + a_1 \tag{9}$$

The expansions for $y_p \sim O(1)$ (outer plume) are

$$\psi = \Psi_b(y_p) + (3\hat{x})^{1/3}\Psi_1(y_p) + \cdots$$
$$H = \Theta_b(y_p) + (3\hat{x})^{1/3}\Theta_1(y_p) + \cdots \quad (10)$$

where

$$\Psi_b' = \sqrt{2}\,(1+\alpha^2)f_b' \quad \text{and} \quad \Theta_b = \theta_b \text{ at } x_b = 1$$

Similarly, the governing equations for the Ψ and Θ can be obtained from Eqs. (10) and (2). They are

$$\Psi_b'\Psi_1' - \Psi_b''\Psi_1 = 0$$
$$\Psi_b'\Theta_1 - \Psi_1'\Theta_b = 0 \quad (11)$$

The solutions of Eqs. (11) are

$$\Psi_1 = a_1\lambda^{-1/3}\Psi_b'(y_p)$$
$$\Theta_1 = a_1\lambda^{-1/3}\Theta_b' \quad (12)$$

in order to match with the inner plume. It is obvious that the structure of the solution for a plume above a wedge is identical to that above a vertical plate. Its solution can be found in Ref. 16 and is not repeated here. The constant a_1 can be determined from the numerical solution of Eqs. (8):

$$a_1 = \lim_{\eta\to\infty}[(2f_0)^{1/2} - \eta] = 0.6185 \quad (13)$$

It is clear from the preceding analysis that the outer plume is the continuation of the natural-convection boundary layers with a small lateral shift. The development of the thin viscous layer, known as the inner plume, is similar to that of a boundary layer near the sharp leading edge of a solid body. The existence of this thin layer is due to the sudden change of the flow boundary condition. Its displacement responds to the lateral shift of the outer plume. In the following section, we will show that the structure of the double decks is consistent with that of the near plume. Consequently, they provide the required initial conditions for the near plume.

It should be noted that the formulation of the near plume in this section is a universally valid solution. This is because its dependence on the boundary-layer velocity profile at $x = 0$ is removed by the transformation. Since the zeroth-order solution of the near plume does not depend on the temperature distribution, it is valid for all Prandtl numbers. It can be shown that buoyancy becomes important only in the far-plume region. This is a consequence of the fact that buoyancy is a cumulative effect. It takes some distance from the location of a change in thermal conditions before the effect of buoyancy reaches an appreciable level.

V. Double-Deck Structure

Since the y component of the velocity in the plume is singular at $\hat{x} = 0$, a double-deck structure is required to join the solutions of the natural-convection boundary layer and the thermal plume. The two-layer structure of the double decks is a consequence of the two-layer structure of the near plume. In the main deck, the flow is inviscid and rotational. The induced pressure gradient in this layer can have an upstream influence. The lower deck is a thin viscous layer near the solid surface and the centerline of the plume. This two-layer structure provides the required initial condition for the downstream plume in order to remove the singularity at $\hat{x} = 0$.

The lateral dimension of the main deck is about the thickness of the boundary layer. The thickness of the lower deck, the axial extent of the decks, and the magnitudes of the velocity components and pressure in both decks can be determined. It is necessary to satisfy several conditions: mass conservation in both decks, the normal pressure gradient balancing with the inertia force in the main deck, the inertia force, viscous forces and axial pressure gradient being of same order in the lower deck, and the axial-velocity component and pressure being of the same order in both decks. The application of these conditions leads to the conclusion that the dimension of the *main deck* is $\epsilon^{6/7} \times \epsilon$. Thus, the stretched coordinates are

$$x_1 = \frac{\hat{x}}{\epsilon^{6/7}}$$
$$y_1 = \frac{\hat{y}}{\epsilon} = y_b \quad (14)$$

The expansions of the dependent variables are

$$\hat{u} = \Psi_b'(y_1) + \epsilon^{2/7}u_1(x_1, y_1) + \cdots$$
$$\hat{v} = \epsilon^{3/7}v_1(x_1, y_1) + \cdots$$
$$\hat{p} = \epsilon^{4/7}p_1(x_1, y_1) + \cdots$$
$$\hat{\theta} = \Theta_b(y_1) + \epsilon^{2/7}\theta_1(x_1, y_1) + \cdots \quad (15)$$

The equations governing the preceding dependent variables can be derived from Eqs. (2). They are

$$\frac{\partial u_1}{\partial x_1} + \frac{\partial v_1}{\partial y_1} = 0$$
$$\Psi_b'\frac{\partial u_1}{\partial x_1} + \Psi_b''v_1 = 0$$
$$\Psi_b'\frac{\partial v_1}{\partial x_1} = -(1+\alpha^2)\frac{\partial p_1}{\partial y_1}$$
$$\Psi_b'\frac{\partial \theta_1}{\partial x_1} + \theta_b'v_1 = 0 \quad (16)$$

The solutions of the preceding equations can be expressed as

$$u_1 = \Psi_b''(y_1)A_1(x_1)$$
$$v_1 = -\Psi_b'(y_1)A_1'(x_1)$$
$$p_1 = -\frac{A_1''(x_1)}{1+\alpha^2}\int_{y_1}^{\infty}[\Psi_b'(y_1)]^2\,dy_1$$
$$\theta_1 = \theta_b'(y_1)A_1(x_1) \quad (17)$$

A *lower deck* is needed since the solution of Eq. (17) does not satisfy the wall condition on the cylinder. The thickness of the lower deck is $O(\epsilon^{9/7})$. Therefore, $\hat{y} = \epsilon^{9/7}\gamma^{1/7}\lambda_1^{-4/7}y$, and the expansions of the dependent variables, which match with the variables of the surrounding regions, are

$$\hat{u} = \epsilon^{2/7}\gamma^{1/7}\lambda_1^{3/7}u(x, y) + \cdots$$
$$\hat{v} = \epsilon^{5/7}\gamma^{-1/7}\lambda_1^{4/7}v(x, y) + \cdots$$
$$\hat{p} = \epsilon^{4/7}\gamma^{2/7}\lambda_1^{6/7}p(x, y) + \cdots$$
$$\hat{\theta} = 1 + \epsilon^{2/7}\gamma^{1/7}\lambda_1^{-4/7}\mu_1\theta(x, y) + \cdots$$
$$A_1 = \gamma^{1/7}\lambda^{-4/7}A(x) \quad (18)$$

where $x = \gamma^{-3/7}\lambda_1^{5/7}x_1$ and $\gamma = \int_0^{\infty}\Psi_b'^2\,dy_1$. Substitution of Eqs. (18) into Eqs. (2) gives

$$\frac{\partial u}{\partial x} + \frac{\partial v}{\partial y} = 0$$
$$u\frac{\partial u}{\partial x} + v\frac{\partial u}{\partial y} = -\frac{1}{1+\alpha^2}\frac{\partial p}{\partial x} + (1+\alpha^2)\frac{\partial^2 u}{\partial y^2}$$

$$\frac{\partial p}{\partial y} = 0$$

$$u\frac{\partial \theta}{\partial x} + v\frac{\partial \theta}{\partial y} = \frac{(1+\alpha^2)}{Pr}\frac{\partial^2 \theta}{\partial y^2} \tag{19}$$

The expansions of Eqs. (19) must match with the boundary-layer solution as $x \to -\infty$ so that

$$u \to y \quad \text{and} \quad \theta \to y \tag{20}$$

As $y \to \infty$, they must also match with the main deck:

$$u \to y + A(x) \quad \text{and} \quad \theta \to y + A(x) \tag{21}$$

On the surface of the cylinder, where $y = 0$ and $x < 0$, the wall conditions are

$$u = v = \theta = 0 \tag{22}$$

and

$$v = \frac{\partial u}{\partial y} = \frac{\partial \theta}{\partial y} = 0 \tag{23}$$

are applied along $y = 0$ for $x > 0$. Finally, since the normal pressure gradient vanishes across the lower deck,

$$p = p_1(y = 0) = \frac{-1}{(1+\alpha^2)}A''(x) \tag{24}$$

Physically, $A(x)$ represents the displacement effect of the lower deck. The main-deck solution matches with the boundary-layer solution as $x \to -\infty$ and with the outer plume as $x \to \infty$. This implies that

$$A(-\infty) \to 0 \quad \text{and} \quad A(\infty) \to a_1(3x)^{1/3} \tag{25}$$

As shown in Eq. (24), the pressure is induced by the change of the lower-deck displacement, which is a consequence of geometric variation. The induced pressure transmits the geometric change upstream and causes the adjustment of the flows in the double decks and further change of the lower-deck displacement. This verifies the elliptic nature of the double decks.

Similarly to the near plume, buoyancy is a smaller-order effect due to the short extent of the double decks. The lower-deck solution previously formulated does not depend on Pr and is a function of the wedge angle. The temperature distribution in the lower deck varies, however, for different Pr.

VI. Results and Discussion

The numerical method used to solve the double-deck equations is almost identical to the one used in Ref. 16. The only difference is that algebraic transformations[21] have been used to map the semi-infinite domain to a finite one. A central-difference scheme is used for derivatives with respect to y, and a three-point backward scheme is used for x derivatives. The scheme is therefore second-order accurate. The grid size of 0.01 was selected after several tests with larger and smaller sizes. The results are believed to be accurate to the third decimal point.

Since the governing equations, Eqs. (19), are different for $x < 0$ and $x > 0$, they have to be solved separately and then matched at $x = 0$. This provides no extra difficulty since Eqs. (19) are parabolic differential equations. Equation (24), a two-point boundary-value problem, requires special attention. The continuity of the displacement $A(x)$ and its derivative is enforced in obtaining the numerical solution.

For $x \to -\infty$, the solution asymptotically approach

$$u \to y + b\psi'(y)e^{\kappa x}$$

$$v \to -b\psi(y)e^{\kappa x}$$

$$p \to -0.8972b\kappa e^{\kappa x}$$

$$\theta \to y + bh(y)e^{\kappa x}$$

$$A \to be^{\kappa x} \tag{26}$$

where $\kappa = 0.8972(1+\alpha^2)$. The equation

$$\psi^{(IV)} - \frac{\kappa}{1+\alpha^2}y\psi''' = 0$$

$$\frac{1}{Pr}h'' - \frac{\kappa}{1+\alpha^2}yh = -\frac{\kappa}{1+\alpha^2}\psi \tag{27}$$

is satisfied by $\psi(y)$ and $h(y)$. The required conditions are

$$y = 0, \qquad \psi = \psi' = h = 0, \qquad \psi''' = -0.8972^3$$

and

$$y \to \infty, \qquad \psi' = h \to 1 \tag{28}$$

Numerical iteration starts at a selected $x_{-\infty}$ with a guessed b. The value of b is adjusted until the boundary condition at x_∞ is satisfied. For large α, it is necessary to choose a smaller value of $x_{-\infty}$. This is because the range of upstream influence decreases as α increases, as indicated by Eq. (26). The numerical solution has been obtained for ϕ up to 85 deg. There is no reason why the solution for even larger ϕ cannot be obtained, but Eq. (19) is obviously not valid for $\phi = 90$ deg, and the upstream influence completely disappears in this limit.

Since the detailed discussion of the double-deck flow structure can be found in Ref. 18, we will concentrate our effort on the thermal field. The modification of the local thermal field is much more complex than that of the flowfield. This is simply because the temperature distribution depends on the Prandtl number. Since the y direction is not normal to the surface, the heat-transfer rate can be calculated in terms of the projection of the temperature derivative along the y direction normal to the surface. The averaged Nusselt number then becomes

$$\bar{N}\bar{u} = \epsilon^{-1}(1+\alpha^2)^{1/2}\mu_1\left[\frac{4}{3} + \epsilon^{6/7}\gamma^{3/7}\lambda_1^{-5/7}Q_c\right] \tag{29}$$

where

$$Q_c = \int_{-\infty}^{0}\left(\frac{\partial \theta}{\partial y} - 1\right)dx \tag{30}$$

It is clear that the double-deck contribution is of $O(\epsilon^{6/7})$ compared with that of the natural-convection boundary layer and is larger than those due to the leading edge, the boundary-layer displacement effects, and the wake effects. On the other hand, the numerical values of γ, λ_1, μ_1, and Q_c listed in Table 1 indicate that the actual contribution is rather small.

In spite of its small contribution to the total heat flux, the modification of the local heat flux cannot be ignored. In Fig. 4, the temperature gradient along the y direction is plotted for $Pr = 0.01$, 0.1, 1, and 10 with $\phi = 30$ deg and for $Pr = 1$ with $\phi = 0$, 30, and 60 deg. The larger temperature gradient for smaller ϕ is due to the longer upstream influence as well as the stronger buoyancy force. Since the boundary-layer thickness is somewhat inversely proportional to Pr, the change of the temperature gradient is larger for a thinner boundary layer. The recovery centerline temperature of the plume is also plotted in Fig. 4. The results show that the centerline temperature recovers much faster for a thick boundary layer (or small Pr) than for a thin boundary layer. It is insensitive to wedge angles.

Typical distributions of horizontal velocity profiles and temperatures near the wedge surface ($x < 0$) and the centerline

Table 1 Coefficients for heat transfer and wall shear

ϕ	Pr	γ	λ_1	$-\mu_1$	Q_c	τ_c
0 deg	0.01	8.8934	1.3969	0.0569	0.0531	0.4332
	0.1	2.3705	1.2150	0.1627	0.0871	
	1.0	0.5200	0.9082	0.4010	0.1307	
	10.0	0.1027	0.5928	0.8268	0.1660	
30 deg	0.01	8.2757	0.9750	0.0459	0.3075×10^{-1}	0.2476
	0.1	2.2060	0.8480	0.1312	0.5030	
	1.0	0.4839	0.6339	0.3232	0.7548	
	10.0	0.0956	0.4137	0.6664	0.9585	
60 deg	0.01	6.1129	0.2468	0.0202	0.3546×10^{-2}	0.2797×10^{-1}
	0.1	1.6762	0.2148	0.0575	0.5812	
	1.0	0.3677	0.1605	0.1418	0.8717	
	10.0	0.0726	0.1048	0.2923	0.1107×10^{-1}	
85 deg	0.01	1.2608	0.0030	0.0021	0.3488×10^{-5}	0.2711×10^{-4}
	0.1	0.6621	0.0027	0.0042	0.5687	
	1.0	0.1535	0.0020	0.0103	0.8529	
	10.0	0.0303	0.0013	0.0213	0.1084×10^{-4}	

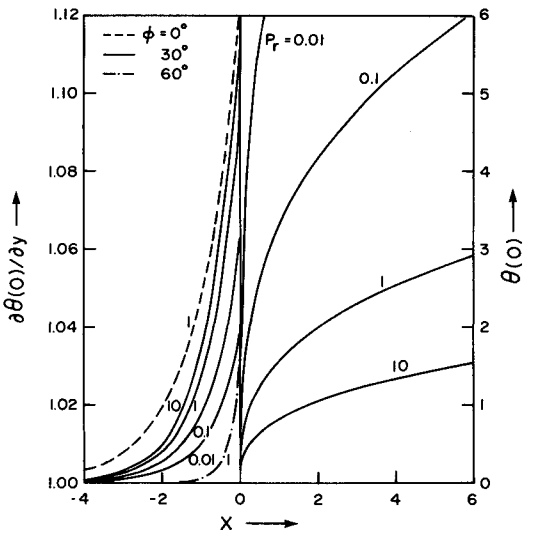

Fig. 4 Heat flux and centerline temperature.

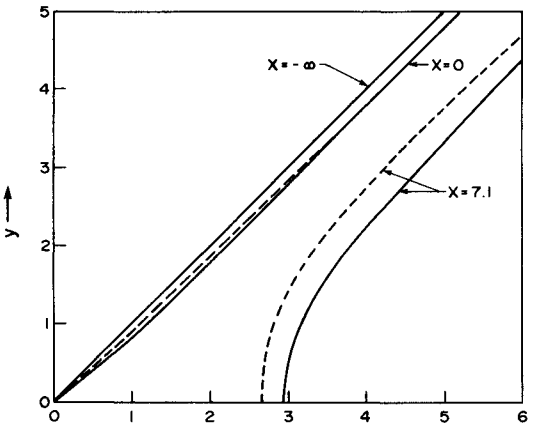

Fig. 5 Lower-deck velocity (——) and temperature (---) distributions for ϕ = 30 deg and Pr = 1.

($x > 0$) of the plume are plotted in Fig. 5 for $\phi = 30$ deg and $Pr = 1$. Far upstream, $x \to \infty$ and both distributions are a straight line [see Eq. (20)].

At the tip of the wedge, the fluid is accelerated due to the favorable pressure gradient induced by the viscous-inviscid interaction in the double deck. Consequently, temperature distribution is modified, resulting in a larger local heat flux. The lower-deck temperature distribution approaches the main-deck solution at a larger y location than that of the velocity profile. This is because the momentum transfer is influenced by the induced pressure gradient. The distance between the solution at $x = -\infty$ and 0 for large y represents the lower-deck displacement [see Eq. (21)].

Far downstream in the plume, $x = 7.1$. Both distributions satisfy the symmetry condition along the centerline and approach the main-deck profiles. The double-deck structure in the plume region is very similar to that of the near-plume solution. It is worthy to note that the solution is regular at $x = 0$. This is because the viscous-inviscid interaction occurring in the double decks allows a large pressure gradient to be established over a relatively short axial distance. The mechanism is in contrast with the classical boundary-layer theory for which the pressure rises gradually and is solely determined by the inviscid flow. This demonstrates that the double-deck solution can indeed smoothly join together the solutions of the natural-convection boundary layer and the near plume.

Similarly, the drag on one side of the wedge, obtained by integrating the perturbation of the wall shear stress from the boundary-layer solution, can be expressed in terms of the velocity gradient in the y direction:

$$\tau = \epsilon^{-1}(1+\alpha^2)^{1/2}\,[0.8\lambda_1 + \epsilon^{6/7}\gamma^{3/7}\lambda_1^{2/7}\tau_c] \tag{31}$$

where

$$\tau_c = \int_{-\infty}^{0}\left(\frac{\partial u}{\partial y} - 1\right)\mathrm{d}x \tag{32}$$

The values of τ_c are also listed in Table 1. In contrast to the limited effect of the thermal field, the trailing edge has a non-negligible contribution to the total drag.

The collision of two inclined viscous layers driven by buoyancy has been described. The extra heat flux induced by the geometric discontinuity at the trailing edge contributes little to

the total heat-transfer rate but substantially modifies the local heat flux. The flow structure, which describes how a viscous layer collides with another or with a solid wall, provides a proper matching principle between two viscous layers upstream and downstream of the collision point. The solutions for these viscous layers can then be confidently calculated by a marching technique, since their governing equations are parabolic differential equations. This provides a reliable way of estimating the total heat flux if one does not care about an accurate prediction of the local heat flux. The double-deck solution presented in this paper indicates that the matching of a downstream viscous layer with an upstream layer can be simply achieved by aligning them. This is how the natural-convection boundary layer along a wedge provides an initial condition for the downstream plume. It is believed that the same matching principle can be applied to other flows.

References

[1]Howarth, L., "Note on the Boundary Layer on a Spinning Sphere," *Philosophical Magazine*, Vol. 42, 1951, pp. 1308–1315.

[2]Dennis, S. C. R., Singh, S. N., and Ingham, D. B., "The Steady Flow due to a Rotating Sphere at Low and Moderate Reynolds Numbers," *Journal of Fluid Mechanics*, Vol. 101, 1980, pp. 257–279.

[3]Amato, W. S. and Tien, C., "Free Convection Heat Transfer from Isothermal Spheres in Water," *International Journal of Heat Mass Transfer*, Vol. 15, 1972, pp. 327–338.

[4]Pera, L. and Gebhart, B., "Experimental Observations of Wake Formation over Cylindrical Surface in Natural Convection Flows," *International Journal of Heat Mass Transfer*, Vol. 15, 1972, pp. 175–177.

[5]Merkin, J. H., "Free Convection Boundary Layers on Cylinders of Elliptic Cross Section," *Journal of Heat Transfer*, Vol. 99, 1977, pp. 453–457.

[6]Yao, L. S. and Berger, S. A., "Entry Flow in a Curved Pipe," *Journal of Fluid Mechanics*, Vol. 67, 1975, pp. 177–196.

[7]Stewartson, K., "On the Flow near the Trailing Edge of a Flat Plate II, " *Mathematika*, Vol. 16, 1969, pp. 106–121.

[8]Stewartson, K., Cebeci, T., and Chang, K. C., "A Boundary-Layer Collision in a Curved Duct," *Quarterly Journal of Mechanics and Applied Mathematics*, Vol. 33, 1980, pp. 59–75.

[9]Yao, L. S., "Entry Flow in a Heated Tube," *Journal of Fluid Mechanics*, Vol. 88, 1978, pp. 465–483.

[10]Messiter, A. F., "The Vertical Plate in Laminar Free Convection," *Journal of Applied Mathematics and Physics* (ZAMP), Vol. 27, 1976, pp. 633–651.

[11]Smith, F. T. and Duck, P. W., "Separation of Jets or Thermal Boundary Layers from a Wall," *Quarterly Journal of Mechanics and Applied Mathematics*, Vol. 30, 1977, pp. 143–156.

[12]Yang, K. T., "Laminar Free-Convection Wake above a Heated Vertical Plate," *Journal of Applied Mechanics*, Vol. 31, 1964, pp. 131–138.

[13]Stewartson, K. and Simpson, C. J., "On a Singularity Initiating a Boundary-Layer Collision," *Quarterly Journal of Mechanics and Applied Mathematics*, Vol. 35, 1982, pp. 1–16.

[14]Messiter, A. F., "Boundary-Layer Flow near the Trailing Edge of a Flat Plate," *SIAM Journal of Applied Mathematics*, Vol. 18, 1970, pp. 241–257.

[15]Smith, F. T., "A Note on a Wall Jet Negotiating a Trailing Edge," *Quarterly Journal of Mechanics and Applied Mathematics*, Vol. 31, 1978, pp. 473–479.

[16]Yang, R. and Yao, L. S., "Natural Convection along a Finite Vertical Plate," to appear in *Journal of Heat Transfer*, 1987.

[17]Merkin, J. H. and Smith, F. T., "Free Convection Boundary Layers Near Corners and Sharp Trailing Edge." *Journal of Applied Mathematics and Physics* (ZAMP), Vol. 33, 1982, pp. 36–52.

[18]Yao, L. S., "A Weak Collision of Two Natural-Convection Boundary Layers," *International Journal of Heat Mass Transfer* (to be published).

[19]Yao, L. S., "A Note on Prandtl's Transposition Theorem," *Journal of Heat Transfer* (to be published).

[20]Yao, L. S., "Natural Convection along a Vertical Wavy Surface," *Journal of Heat Transfer*, Vol. 105, 1983, pp. 465–468.

[21]Dijkstra, D., "Separating, Incompressible, Laminar Boundary-Layer Flow over a Smooth Step of Small Height," *Proceedigns of the 6th International Conference on Numerical Methods Fluid Dynamics*, 1978, pp. 169–176.

[22]Goldstein, S., "Concerning Some Solutions of the Boundary-Layer Equations in Hydrodynamics," *Proceedings of the Cambridge Philosophical Society*, Vol. 26, 1929, pp. 1–30.